Nonlinear Dyn (2012) 67:1031–1041
DOI 10.1007/s11071-011-0045-z

ORIGINAL PAPER

# Inverse dynamics of a 3-PRC parallel kinematic machine

**Yangmin Li · Stefan Staicu**

Received: 20 March 2011 / Accepted: 5 April 2011 / Published online: 6 May 2011


**Abstract** Recursive matrix relations for kinematics and dynamics analysis of a three-prismatic-revolute-cylindrical (3-PRC) parallel kinematic machine (PKM) are performed in this paper. Knowing the translational motion of the platform, we develop first the inverse kinematical problem and determine the positions, velocities and accelerations of the robot's elements. Further, the inverse dynamic problem is solved using an approach based on the principle of virtual work and the results in the framework of the Lagrange equations with their multipliers can be verified. Finally, compact matrix equations and graphs of simulation for input force and power of each of three actuators are obtained. The investigation of the dynamics of this parallel mechanism is made mainly to solve successfully the control of the motion of such robotic system.

**Keywords** Dynamics modelling · Kinematics · Lagrange equations · Parallel kinematic machine · Virtual work

Y. Li (✉)
Department of Electromechanical Engineering, University of Macau, Taipa, Macao SAR, China
e-mail: ymli@umac.mo

S. Staicu
Department of Mechanics, University "Politehnica" of Bucharest, Bucharest, Romania
e-mail: staicunstefan@yahoo.com

**Nomenclature**

| | |
|---|---|
| $a_{k,k-1}, b_{k,k-1}, c_{k,k-1}$ | orthogonal transformation matrices |
| $\theta_1, \theta_2$ | two constant orthogonal matrices |
| $\vec{u}_1, \vec{u}_2, \vec{u}_3$ | three right-handed orthogonal unit vectors |
| $l = 2r\sqrt{3}$ | length of the side of moving platform |
| $l_2$ | length of the limb of each leg |
| $\theta$ | angle of inclination of three sliders |
| $\lambda_{10}^A, \lambda_{10}^B, \lambda_{10}^C$ | displacements of three prismatic actuators |
| $\varphi_{k,k-1}$ | relative rotation angle of $T_k$ rigid body |
| $\vec{w}_{k,k-1}$ | relative angular velocity of $T_k$ |
| $\vec{w}_{k0}$ | absolute angular velocity of $T_k$ |
| $\tilde{w}_{k,k-1}$ | skew-symmetric matrix associated to the angular velocity $\vec{w}_{k,k-1}$ |
| $\vec{\varepsilon}_{k,k-1}$ | relative angular acceleration of $T_k$ |
| $\vec{\varepsilon}_{k0}$ | absolute angular acceleration of $T_k$ |
| $\tilde{\varepsilon}_{k,k-1}$ | skew-symmetric matrix associated to the angular acceleration $\vec{\varepsilon}_{k,k-1}$ |
| $\vec{r}_{k,k-1}^A$ | relative position vector of the centre $A_k$ of joint |
| $\vec{v}_{k,k-1}^A$ | relative velocity of the centre $A_k$ |
| $\vec{\gamma}_{k,k-1}^A$ | relative acceleration of the centre $A_k$ |
| $\vec{r}_k^C$ | position vector of the mass centre of $T_k$ rigid body |
| $m_k, \hat{J}_k$ | mass and symmetric matrix of tensor of inertia of $T_k$ about the link-frame $x_k y_k z_k$ |
| $f_{10}^A, f_{10}^B, f_{10}^C$ | input forces of prismatic actuators |

## 1 Introduction

Recently, the research activities on parallel mechanisms have gained greater attention for engineers within the robotic community as their advantages have become better known. Parallel kinematic machines (PKM) are closed-loop structures presenting a very good potential in terms of accuracy, rigidity and ability to manipulate large loads. In general, these mechanisms consist of two main bodies coupled via numerous legs acting in parallel. One body is designated as fixed and is called *base*, while the other is regarded as movable and hence is called a *moving platform* of the manipulator. The number of actuators is typically equal to the number of degrees of freedom such that each leg is controlled at or near the fixed base [1].

Compared with traditional serial manipulators, the followings are the potential advantages of parallel architectures: higher kinematical accuracy, lighter weight and better structural rigidity, stable capacity and suitable position of arrangement of actuators, low manufacturing cost and better payload carrying ability. But, from an application point of view, a limited workspace and complicated singularities are two major drawbacks of parallel manipulators. Thus, it is more suitable for situations where high precision, stiffness, velocity and heavy load-carrying are required within a restricted workspace [2].

Most 3-DOF mechanisms exist in one of three following classes: spherical, translational or spatial. A translational device is capable of moving in Cartesian coordinates and is suitable for pick-and-place applications. Spherical mechanisms are often used for configuring applications such as orienting a camera. The class of spatial mechanisms includes a combination of both rotational and translational degrees of freedom.

Over the past two decades, parallel manipulators have received more attentions from academics and industries. Important companies such as Giddings & Lewis, Ingersoll, Hexel and others have developed them as high precision machine tools. Accuracy and precision in the direction of the tasks are essential since the positioning errors of the tool could end in costly damage.

Considerable efforts have been devoted to the kinematic and dynamic investigations of fully parallel manipulators. Among these, the class of manipulators known as Stewart–Gough platform attracted great attention (Stewart [3], Di Gregorio and Parenti Castelli [4]). They are used in flight simulators and more recently for PKMs.

The prototype of Delta parallel robot (Clavel [5], Tsai and Stamper [6], Staicu [7]) developed by Clavel at the Federal Polytechnic Institute of Lausanne and by Tsai and Stamper at the University of Maryland as well as the Star parallel manipulator (Hervé and Sparacino [8]) are equipped with three motors, which train on the mobile platform in a three-degrees-of-freedom general translation motion. Angeles [9], Wang and Gosselin [10], Staicu [11] analysed the kinematics, dynamics and singularity loci of Agile Wrist spherical robot with three actuators.

Ordinarily, there are two problems in PKM dynamics, namely the forward and inverse dynamics, where the latter solves the input forces of actuators once the motions of the moving platform are planned and can be immediately used for the design of a dynamics controller. As far as the approaches to generate a PKM inverse dynamic model are concerned, most traditional methods are used such as Newton–Euler formulation [12–14], Lagrange formalism [10, 15–17], the principle of virtual work [18–21] and commonly known Kane's method [22]. With respect to the real time control of the PKM, the goal of the dynamic modelling is to establish an inverse dynamic model which is simple yet accurate enough to represent the PKM system. Once the PKM is designed and developed, its manipulation accuracy can be guaranteed by designing a proper controller. The inverse dynamic control (IDC) can produce a nice control performance, provided that a full dynamic model of the PKM is used with all dynamic parameters known exactly [23, 24].

In the present paper, a recursive matrix method, already implemented in the inverse dynamics of parallel robots, is applied to the analysis of the spatial three-degrees-of-freedom mechanism. It has been proved to reduce the number of equations and computation operations significantly by using a set of matrices for kinematic and dynamic models. Therefore, we employ an exact dynamic model in conjunction with a robust controller to seek for an effective approach to deal with the control issues for a PKM in this research.

## 2 Kinematic analysis

In the previous works of Li and Xu [25–27], the 3-PRS parallel manipulator and the 3-PRC PKM with rela-

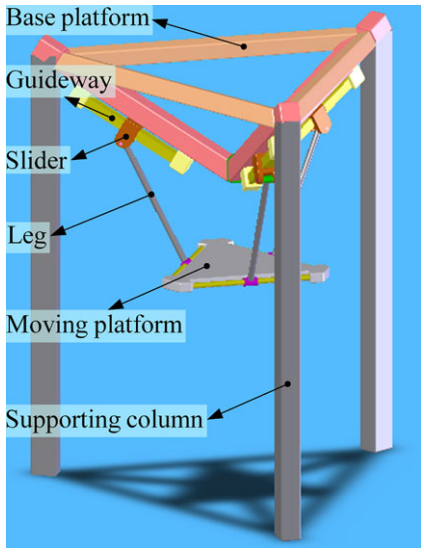


**Fig. 1** A virtual prototype of the 3-PRC PKM

tive simple structure were presented with their kinematic problems solved in details. The potential application as a positioning device of the tool in a new parallel kinematic machine for high precision blasting attracted a scientific and practical interest to this manipulator type.

Having a closed-loop structure, the spatial 3-PRC parallel kinematic machine is a special symmetrical mechanism composed of three kinematical chains with identical topology, all connecting the fixed base to the moving platform (Fig. 1). Each limb connects the moving platform to the base by a prismatic joint, axe of which is being inclined from the base platform, a revolute joint and a passive cylindrical joint in sequence, where the prismatic joints are driven by three linear actuators assembled at the fixed base.

Since the kinematics and mobility problems have already been resolved, we only review some matrix useful results below which provide a base for the dynamic modelling. The manipulator consists of the upper fixed base and the moving platform $A_3B_3C_3$ that are two equilateral triangles with $L$ and $l = 2r\sqrt{3}$ the lengths of the sides, respectively. Overall, there are seven moving links, three prismatic joints, three revolute joints and three cylindrical joints. Grübler mobility equation predicts that the device has certainly three degrees of freedom. Practically, the degree-of-freedom value $F = 3$ of the mechanism is equal to the degrees of freedom associated with all the moving links $\nu = 12$, minus the total number of independent constraint relations $l = 9$ imposed by the joints.

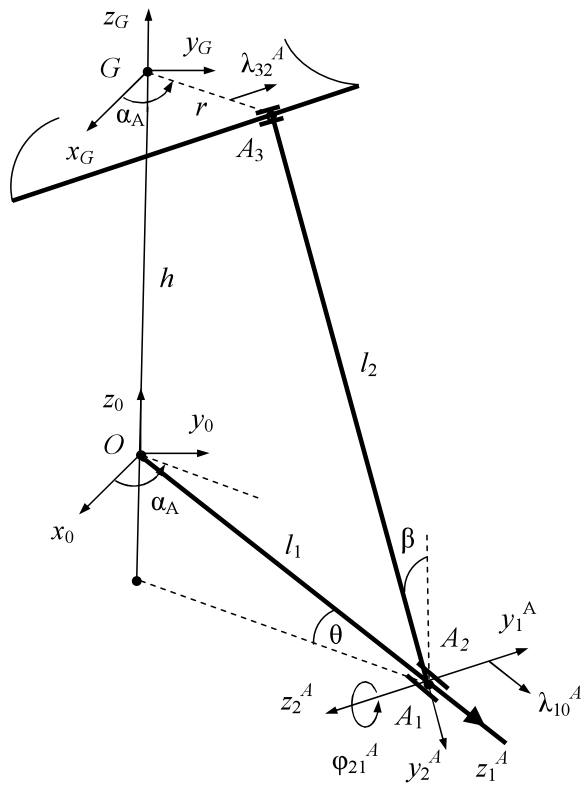


**Fig. 2** Kinematical scheme of the first leg $A$ of upside-down mechanism

In the configuration ($\underline{P}RC$) with all actuators installed on the fixed base, we consider the moving platform as the output link and the sliders $A_1, B_1, C_1$ as the input links (Fig. 2). Having a common point of intersection $O$, the lines of action of each of three prismatic joints may be inclined from the fixed base by a constant angle $\theta$ as architectural parameter. These rails and the revolute joint axes are mutually perpendicular. Finally, the passive revolute joint of each leg is separated from the cylindrical joint connecting the platform's edge by a fixed-length limb. In this configuration, any translation along the vertical axis is limited by the constraints and therefore only finite displacements along this axis are obtained.

For the purpose of analysis, a Cartesian frame $Ox_0y_0z_0(T_0)$ is attached to the fixed base with its origin located just at the common point $O$ of three rails, the $z_0$ axis perpendicular to the base. Another mobile reference frame $Gx_Gy_Gz_G$ is attached to the moving platform. The origin of this coordinate central system

is fixed at the centre $G$ of the moving triangle. The kinematical constraints of each leg limit the *absolute motion* of cylindrical joint of each limb to a plane perpendicular to the axis of the revolute joint and containing the rail. In the symmetrical version of the manipulator, the first leg $A$ is typically contained within the $Ox_0z_0$ vertical plane, whereas the remaining two legs $B, C$ make angles $\alpha_B = 120°$, $\alpha_C = -120°$, respectively, with the first leg. It is noted that the relative rotation with $\varphi_{k,k-1}$ angle or relative translation of $T_k$ body with $\lambda_{k,k-1}$ displacement must be always pointing about or along the direction of $z_k$ axis.

In what follows we consider that the moving platform is initially located at a *central configuration*, where the platform is not translated with respect to the fixed base and the origin $O$ of fixed frame is located at an elevation $OG = h$ above the mass centre $G$. A complete description of the absolute position of the translational moving platform with respect to the reference frame requires generally three variables: the coordinates $x_0^G, y_0^G, z_0^G$ of the mass centre $G$.

One of three active legs (for example, leg $A$) consists of a prismatic joint of mass $m_1$ linked at the $A_1x_1^Ay_1^Az_1^A$ moving frame, having a translation with the displacement $\lambda_{10}^A$, the velocity $v_{10}^A = \dot{\lambda}_{10}^A$ and the acceleration $\gamma_{10}^A = \ddot{\lambda}_{10}^A$. An intermediate link of length $A_2A_3 = l_2$, mass $m_2$ and tensor of inertia $\hat{J}_2$ has a relative rotation about $z_2^A$ axis with the angle $\varphi_{21}^A$, the angular velocity $\omega_{21}^A = \dot{\varphi}_{21}^A$ and the angular acceleration $\varepsilon_{21}^A = \ddot{\varphi}_{21}^A$. Finally, a cylindrical joint is introduced at the edge of a planar moving platform, which is schematised as an equilateral triangle of mass $m_p$ and tensor of inertia $\hat{J}_p$.

At the central configuration, we also consider that the three sliders are initially starting from the same position $OA_1 = l_1 = r\cos\theta - h\sin\theta + l_2\sin(\theta+\beta)$ and that the angles of orientation of the legs are given by

$$\theta = \frac{\pi}{6}, \quad \alpha_A = 0, \quad \alpha_B = \frac{2\pi}{3}, \quad \alpha_C = -\frac{2\pi}{3}, \qquad (1)$$
$$l_2\cos(\theta+\beta) = r\sin\theta + h\cos\theta.$$

In the following, we apply the method of successive displacements to geometric analysis of closed-loop chains. So, starting from the reference origin $O$ and pursuing the independent legs $OA_1A_2A_3$, $OB_1B_2B_3$ and $OC_1C_2C_3$, we obtain the following transformation matrices:

$$p_{10} = a_\theta\theta_1 a_\alpha^i, \quad p_{21} = p_{21}^\varphi a_{\beta\theta}\theta_1\theta_2^T, \quad p_{20} = p_{21}p_{10}$$
$$(p = a, b, c,\ i = A, B, C), \qquad (2)$$

where we denote [28]:

$$a_\alpha^i = \begin{bmatrix} \cos\alpha_i & \sin\alpha_i & 0 \\ -\sin\alpha_i & \cos\alpha_i & 0 \\ 0 & 0 & 1 \end{bmatrix},$$

$$a_{\beta\theta} = \begin{bmatrix} \cos(\theta+\beta) & \sin(\theta+\beta) & 0 \\ -\sin(\theta+\beta) & \cos(\theta+\beta) & 0 \\ 0 & 0 & 1 \end{bmatrix},$$

$$a_\theta = \begin{bmatrix} \cos\theta & 0 & -\sin\theta \\ 0 & 1 & 0 \\ \sin\theta & 0 & \cos\theta \end{bmatrix}, \qquad (3)$$

$$p_{21}^\varphi = \begin{bmatrix} \cos\varphi_{21}^i & \sin\varphi_{21}^i & 0 \\ -\sin\varphi_{21}^i & \cos\varphi_{21}^i & 0 \\ 0 & 0 & 1 \end{bmatrix},$$

$$\theta_1 = \begin{bmatrix} 0 & 0 & -1 \\ 0 & 1 & 0 \\ 1 & 0 & 0 \end{bmatrix}, \qquad \theta_2 = \begin{bmatrix} 0 & 1 & 0 \\ -1 & 0 & 0 \\ 0 & 0 & 1 \end{bmatrix}.$$

Three independent displacements $\lambda_{10}^A, \lambda_{10}^B, \lambda_{10}^C$ of the active links are the joint variables that give the input vector $\vec{\lambda}_{10} = [\lambda_{10}^A\ \lambda_{10}^B\ \lambda_{10}^C]^T$ of the instantaneous pose of the mechanism. But, in the inverse geometric problem, it can be considered that the position of the mechanism is completely given through the coordinate $x_0^G, y_0^G, z_0^G$ of the mass centre $G$. Further, we suppose that the following three analytical functions can describe a *helical* translation of the moving platform [29]:

$$x_0^G = d\sin(\omega_1 t)\cos(\omega_2 t),$$
$$y_0^G = d\sin(\omega_1 t)\sin(\omega_2 t), \qquad (4)$$
$$z_0^G = h + de[1-\cos(\omega_1 t)],$$

where $d = 0.5$, $e = 0.5$, $\omega_1 = \frac{\pi}{2}$, $\omega_2 = 3\omega_1$, $t$ is the time variable in seconds and $x_0^G, y_0^G, z_0^G$ are the coordinates of the centre $G$ in metres.

Nine independent variables $\lambda_{10}^A, \varphi_{21}^A, \lambda_{32}^A, \lambda_{10}^B, \varphi_{21}^B, \lambda_{32}^B, \lambda_{10}^C, \varphi_{21}^C, \lambda_{32}^C$ will be determined by several vector-loop equations as follows:

$$\begin{aligned}
&\vec{r}_{10}^{\,A} + \sum_{k=1}^{2} a_{k0}^{T}\vec{r}_{k+1,k}^{\,A} - \vec{r}_{G}^{\,A_3} \\
&\quad = \vec{r}_{10}^{\,B} + \sum_{k=1}^{2} b_{k0}^{T}\vec{r}_{k+1,k}^{\,B} - \vec{r}_{G}^{\,B_3} \\
&\quad = \vec{r}_{10}^{\,C} + \sum_{k=1}^{2} c_{k0}^{T}\vec{r}_{k+1,k}^{\,C} - \vec{r}_{G}^{\,C_3} = \vec{r}_{0}^{\,G},
\end{aligned} \tag{5}$$

where

$$\begin{aligned}
&\vec{u}_1 = \begin{bmatrix}1\\0\\0\end{bmatrix}, \qquad \vec{u}_2 = \begin{bmatrix}0\\1\\0\end{bmatrix}, \qquad \vec{u}_3 = \begin{bmatrix}0\\0\\1\end{bmatrix}, \\
&\tilde{u}_3 = \begin{bmatrix}0 & -1 & 0\\ 1 & 0 & 0\\ 0 & 0 & 0\end{bmatrix}, \\
&\vec{r}_{10}^{\,i} = \big(l_1 + \lambda_{10}^{i}\big)p_{10}^{T}\vec{u}_3, \qquad \vec{r}_{21}^{\,i} = \vec{0}, \\
&\vec{r}_{32}^{\,i} = -l_2\vec{u}_2, \\
&\vec{r}_{G}^{\,i_3} = \big[r\cos\alpha_i - \lambda_{32}^{i}\sin\alpha_i \;\; r\sin\alpha_i - \lambda_{32}^{i}\cos\alpha_i \;\; 0\big]^{T} \\
&\quad (i = A, B, C).
\end{aligned} \tag{6}$$

Actually, these vector equations mean that there is only one inverse geometric solution for the spatial manipulator:

$$\begin{aligned}
&l_2\cos\big(\varphi_{21}^{i} + \theta + \beta\big) \\
&\quad = \big(r + x_0^G\cos\alpha_i + y_0^G\sin\alpha_i\big)\sin\theta + z_0^G\cos\theta, \\
&\lambda_{10}^{i} = l_2\sin\big(\varphi_{21}^{i} + \theta + \beta\big) \\
&\quad + \big(r + x_0^G\cos\alpha_i + y_0^G\sin\alpha_i\big)\cos\theta - z_0^G\sin\theta - l_1, \\
&\lambda_{32}^{i} = x_0^G\sin\alpha_i - y_0^G\cos\alpha_i.
\end{aligned} \tag{7}$$

Now, we develop the inverse kinematic problem and determine the velocities and accelerations of the robot, supposing that the motion of the moving platform is known. The motions of the compounding elements of the leg $A$, for example, are characterised by the velocities of joints

$$\vec{v}_{10}^{\,A} = \dot{\lambda}_{10}^{A}\vec{u}_3, \qquad \vec{v}_{21}^{\,A} = \vec{0}, \qquad \vec{v}_{20}^{\,A} = a_{21}\vec{v}_{10}^{\,A} \tag{8}$$

and by the following angular velocities:

$$\vec{\omega}_{10}^{\,A} = \vec{0}, \qquad \vec{\omega}_{20}^{\,A} = \vec{\omega}_{21}^{\,A} = \dot{\varphi}_{21}^{A}\vec{u}_3, \tag{9}$$

which are *associated* to skew-symmetric matrices

$$\tilde{\omega}_{10}^{\,A} = \tilde{0}, \qquad \tilde{\omega}_{20}^{\,A} = \tilde{\omega}_{21}^{\,A} = \dot{\varphi}_{21}^{A}\tilde{u}_3. \tag{10}$$

Vector equations of geometrical constraints (5) can be differentiated with respect to time to obtain the following significant *matrix conditions of connectivity* [30]:

$$\begin{aligned}
&v_{10}^{A}\vec{u}_j^{\,T}a_{10}^{T}\vec{u}_3 + \omega_{21}^{A}\vec{u}_j^{\,T}a_{20}^{T}\tilde{u}_3\vec{r}_{32}^{\,A} - v_{32}^{A}\vec{u}_j^{\,T}a_{\alpha}^{AT}\vec{u}_2 = \vec{u}_j^{\,T}\dot{\vec{r}}_{0}^{\,G} \\
&\quad (j = 1, 2, 3).
\end{aligned} \tag{11}$$

If the other two kinematical chains of the robot are pursued, analogous relations can be easily obtained.

From these equations we obtain the *complete* Jacobian matrix of the manipulator. This matrix is a fundamental element for the analysis of the robot workspace and the particular configurations of singularities where the spatial manipulator becomes uncontrollable [31].

Rearranging, the above constraint equations (7) can immediately be written as

$$\begin{aligned}
&\big[\big(r + x_0^G\cos\alpha_i + y_0^G\sin\alpha_i\big)\sin\theta + z_0^G\cos\theta\big]^2 \\
&\quad + \big[\lambda_{10}^{i} + l_1 - \big(r + x_0^G\cos\alpha_i + y_0^G\sin\alpha_i\big)\cos\theta \\
&\quad + z_0^G\sin\theta\big]^2 = l_2^2 \quad (i = A, B, C).
\end{aligned} \tag{12}$$

The derivative with respect to time of conditions (12) leads to the matrix equation

$$J_1\dot{\vec{\lambda}}_{10} = J_2\big[\dot{x}_0^G \;\; \dot{y}_0^G \;\; \dot{z}_0^G\big]^{T}, \tag{13}$$

where the matrices $J_1$ and $J_2$ are, respectively, the inverse and forward Jacobian of the manipulator

$$\begin{aligned}
&J_1 = \operatorname{diag}\{\delta_A \;\; \delta_B \;\; \delta_C\}, \\
&J_2 = \begin{bmatrix}\beta_1^A & \beta_2^A & \beta_3^A\\ \beta_1^B & \beta_2^B & \beta_3^B\\ \beta_1^C & \beta_2^C & \beta_3^C\end{bmatrix},
\end{aligned} \tag{14}$$

with the notations

$$\begin{aligned}
&\delta_i = \sin\big(\varphi_{21}^{i} + \theta + \beta\big) \quad (i = A, B, C), \\
&\beta_1^i = \sin\big(\varphi_{21}^{i} + \beta\big)\cos\alpha_i, \\
&\beta_2^i = \sin\big(\varphi_{21}^{i} + \beta\big)\sin\alpha_i, \\
&\beta_3^i = -\cos\big(\varphi_{21}^{i} + \beta\big).
\end{aligned} \tag{15}$$

The three kinds of singularities of the three closed-loop kinematical chains can be determined through the analysis of two Jacobian matrices $J_1$ and $J_2$ [32–34].

The matrix kinematical relations (8)–(11) will be further required in the computation of virtual velocity distribution of the elements of the manipulator. Let us

assume that the manipulator has a first *virtual motion* determined by the linear velocities $v_{10a}^{Av}=1$, $v_{10a}^{Bv}=0$, $v_{10a}^{Cv}=0$. The characteristic *virtual velocities* are expressed as functions of the position of the mechanism by the general kinematical constraint equations (11). These virtual velocities are required for the computation of the virtual work of all forces applied to the component elements of the mechanism.

As for the linear accelerations $\gamma_{10}^{A}, \gamma_{32}^{A}$ and the angular acceleration $\varepsilon_{21}^{A}$ of the first leg $A$, the derivatives with respect to time of (11) give other conditions of connectivity:

$$\begin{aligned}&\gamma_{10}^{A}\vec{u}_j^T a_{10}^T\vec{u}_3+\varepsilon_{21}^{A}\vec{u}_j^T a_{20}^T\tilde{u}_3\vec{r}_{32}^{A}-\gamma_{32}^{A}\vec{u}_j^T a_{\alpha}^{AT}\vec{u}_2\\&\quad=\vec{u}_j^T\dot{\vec{r}}_0^{G}-\omega_{21}^{A}\omega_{21}^{A}\vec{u}_j^T a_{20}^T\tilde{u}_3\tilde{u}_3\vec{r}_{32}^{A}\quad(j=1,2,3).\end{aligned}\tag{16}$$

The following relations give the angular accelerations $\vec{\varepsilon}_{k0}^{A}$ and the accelerations $\vec{\gamma}_{k0}^{A}$ of joints $A_k$:

$$\begin{aligned}&\vec{\varepsilon}_{10}^{A}=\vec{0},\qquad\vec{\varepsilon}_{20}^{A}=\vec{\varepsilon}_{21}^{A}=\ddot{\varphi}_{21}^{A}\vec{u}_3,\\&\vec{\gamma}_{10}^{A}=\ddot{\lambda}_{10}^{A}\vec{u}_3,\qquad\vec{\gamma}_{21}^{A}=\vec{0},\qquad\vec{\gamma}_{20}^{A}=a_{21}\vec{\gamma}_{10}^{A}.\end{aligned}\tag{17}$$

The matrix relations (16) and (17) will be further used for the computation of the wrench of the inertia forces for every rigid component of the robot. The dynamic model of the mechanism would only be established with regard to the complete geometrical analysis and kinematics of the mechanical system

## 3 Dynamic modelling

When a good dynamic performance and a higher accuracy in positioning of the moving platform under large load are required, the dynamic model of the robot is important for the automatic control. Inverse dynamic model is of great significance in the optimisation of sectional parameters of components and estimation of servomotor parameters.

The dynamics of parallel manipulators is complicated by existence of multiple closed-loop chains. Difficulties commonly encountered in dynamics modelling of parallel robots include problematic issues such as: complicated spatial kinematical structure with large number of passive degrees of freedom, dominance of inertial forces over the frictional and gravitational components and the problem linked to the solution of the inverse dynamics.

In the context of the real time control, neglecting the friction forces and considering the gravitational effects, the relevant objective of the dynamics is to determine the input torques or forces which must be exerted by the actuators in order to produce a given trajectory of the end-effector.

A lot of works have focused on the dynamics of Stewart platform. Dasgupta and Mruthyunjaya [13] used the Newton–Euler approach to develop closed-form dynamic equations of Stewart platform, considering all dynamic and gravity effects as well as viscous friction at joints. Tsai [1] presented an algorithm to solve the inverse dynamics for a Stewart platform type using Newton–Euler equations. This commonly known approach requires computation of all constraint forces and moments between the links. Geng et al. [16] developed Lagrange equations of motion under some simplifying assumptions regarding the geometry and inertia distribution of the manipulator. An interesting dynamic modelling is validated by Bi, Lang and Verner for the specific case of a tripod-based machine tool [35].

### 3.1 Principle of virtual work

Knowing the position and kinematic state of each link as well as the external forces acting on the robot, in the present paper we apply the principle of virtual work for the inverse dynamic problem in order to establish some definitive recursive matrix relations. The three input forces and powers required in a given translation motion of the platform will be computed using a recursive procedure.

Three independent mechanical systems, acting with the forces $\vec{f}_{10}^{A}=f_{10}^{A}\vec{u}_3$, $\vec{f}_{10}^{B}=f_{10}^{B}\vec{u}_3$, $\vec{f}_{10}^{C}=f_{10}^{C}\vec{u}_3$ along the directions $z_1^A, z_1^B, z_1^C$ of three rails, control the motion of the moving platform. The parallel robot can artificially be transformed into a set of three open chains $C_i$ $(i=A,B,C)$ subject to the constraints. This is possible by cutting each joint for the moving platform, and takes its effect by introducing the corresponding constraint conditions.

The force of inertia and the resulting moment of the forces of inertia of an arbitrary rigid body $T_k^A$, for example,

$$\begin{aligned}&\vec{f}_{k0}^{\,\mathrm{in}A}=-m_k^A\big[\vec{\gamma}_{k0}^{A}+\big(\tilde{\omega}_{k0}^{A}\tilde{\omega}_{k0}^{A}+\tilde{\varepsilon}_{k0}^{A}\big)\vec{r}_k^{CA}\big],\\&\vec{m}_{k0}^{\,\mathrm{in}A}=-\big[m_k^A\tilde{r}_k^{CA}\vec{\gamma}_{k0}^{A}+\hat{J}_k^A\vec{\varepsilon}_{k0}^{A}+\tilde{\omega}_{k0}^{A}\hat{J}_k^A\vec{\omega}_{k0}^{A}\big]\end{aligned}\tag{18}$$

are determined with respect to the centre of joint $A_k$. On the other hand, the wrench of two vectors $\vec{f}_k^{*A}$ and $\vec{m}_k^{*A}$ evaluates the influence of the action of the weight $m_k^A \vec{g}$ and of other external and internal forces applied to the same element $T_k^A$ of the manipulator:

$$\vec{f}_k^{*A} = m_k^A g a_{k0} \vec{u}_2, \quad \vec{m}_k^{*A} = m_k^A g \tilde{r}_k^{CA} a_{k0} \vec{u}_2 \quad (k = 1, 2). \tag{19}$$

The fundamental principle of the virtual work states that a mechanism is under dynamic equilibrium if and only if the virtual work developed by all external, internal and inertia forces vanishes during any general virtual displacement, which is compatible with the constraints imposed on the mechanism. Assuming that the frictional forces at the joints are negligible, the virtual work produced by all forces of constraint at the joints is zero.

Applying the definitive form of *fundamental equations of parallel robots dynamics* [36, 37], the following compact matrix relations for the input force of first active *prismatic joint* are:

$$f_{10}^A = \vec{u}_3^T \{ \vec{F}_1^A + \omega_{21a}^{Av} \vec{M}_2^A + \omega_{21a}^{Bv} \vec{M}_2^B + \omega_{21a}^{Cv} \vec{M}_2^C + v_{10a}^{Gv} \vec{F}_1^G + v_{21a}^{Gv} \vec{F}_2^G + v_{32a}^{Gv} \vec{F}_3^G \}. \tag{20}$$

Two recursive relations generate the vectors

$$\begin{aligned} \vec{F}_k^A &= \vec{F}_{k0}^A + a_{k+1,k}^T \vec{F}_{k+1}^A, \\ \vec{M}_k^A &= \vec{M}_{k0}^A + a_{k+1,k}^T \vec{M}_{k+1}^A + \tilde{r}_{k+1,k}^A a_{k+1,k}^T \vec{F}_{k+1}^A \end{aligned} \tag{21}$$

where we denote

$$\vec{F}_{k0}^A = -\vec{f}_{k0}^{\,\mathrm{in}A} - \vec{f}_k^{*A}, \qquad \vec{M}_{k0}^A = -\vec{m}_{k0}^{\,\mathrm{in}A} - \vec{m}_k^{*A}. \tag{22}$$

The relations (19)–(22) represent the *inverse dynamics model* of the 3-PRC parallel kinematic machine. These explicit equations are definitively written in a recursive compact form, *only* based on the relative virtual velocities of intensities $v_{k,k-1}^v$ and $\omega_{k.k-1}^v$. The various dynamical effects, including the Coriolis and centrifugal forces coupling and the gravitational actions, are considered. This dynamics model is successfully expected to be deployed for robotic control.

The above compact relations (20) and (21) can be also applied to calculate any internal joint force or joint torque by considering several fictitious displacements or rotations in each joint of the manipulator.

In what follows we can apply the Newton–Euler procedure to establish the set of analytical equations for each compounding rigid body of a prototype manipulator in a real application. These equations give all connecting forces in the external and internal joints. Several relations from the general system of equations could eventually constitute verification for the input forces or active torques obtained by the method based on the principle of virtual work. Now, we can calculate the friction forces and the friction torques in the joints, based on the friction coefficients and the maximum of the connecting forces in the joints. We apply again the explicit equations (20) and (21), where the contribution of the virtual work of friction forces in joints is added. The new active torques and input forces are compared to the values obtained in the first calculus. The present approach can easily be extended to the mechanics analysis of other types of parallel manipulators.

The friction of joints could be also analysed by the approach of Lu, Hu and Yu proposed in their papers on dynamics of limited-DOF parallel manipulators [38, 39].

### 3.2 Lagrange equations

A solution of the dynamics problem of the 3-PRC PKM can be developed based on the Lagrange equations of second kind for a mechanical system with constraints. The generalised coordinates of the robot are represented by nine parameters:

$$\begin{aligned} &q_1 = x_0^G, \quad q_2 = y_0^G, \quad q_3 = z_0^G, \\ &q_4 = \lambda_{10}^A, \quad q_5 = \varphi_{21}^A, \quad q_6 = \lambda_{10}^B, \\ &q_7 = \varphi_{21}^B, \quad q_8 = \lambda_{10}^C, \quad q_9 = \varphi_{21}^C. \end{aligned} \tag{23}$$

The Lagrange equations with their six multipliers $\lambda_1, \lambda_2, \ldots, \lambda_6$ will be expressed by nine differential relations

$$\frac{d}{dt}\left\{\frac{\partial L}{\partial \dot{q}_k}\right\} - \frac{\partial L}{\partial q_k} = Q_k + \sum_{s=1}^{6} \lambda_s c_{sk} \quad (k = 1, 2, \ldots, 9) \tag{24}$$

which contain the following nine generalised forces: $Q_1 = 0$, $Q_2 = 0$, $Q_3 = 0$, $Q_4 = f_{10}^A$, $Q_5 = 0$, $Q_6 = f_{10}^B$, $Q_7 = 0$, $Q_8 = f_{10}^C$, $Q_9 = 0$.

A number of six kinematical constraint conditions are given by the relations (11):

$$\sum_{k=1}^{9} c_{sk} \dot{q}_k = 0 \quad (s = 1, 2, \ldots, 6). \tag{25}$$

The components of the general expression of the Lagrange function $L = L_p + \sum_{\nu=1}^{2}(L_\nu^A + L_\nu^B + L_\nu^C)$ are expressed as analytical functions of the generalised coordinates and their first derivatives with respect to time:

$$
\begin{aligned}
L_p &= \frac{1}{2}m_p\left(\dot{x}_0^{G2} + \dot{y}_0^{G2} + \dot{z}_0^{G2}\right) - m_p g z_0^G,\\
L_1^i &= \frac{1}{2}m_1^i \vec{v}_{10}^{iT}\vec{v}_{10}^i - m_1^i g\vec{u}_3^T\vec{r}_{10}^i,\\
L_2^i &= \frac{1}{2}m_2^i \vec{v}_{20}^{iT}\vec{v}_{20}^i + \frac{1}{2}\vec{\omega}_{20}^{iT}\hat{J}_2^i\vec{\omega}_{20}^i + m_2^i\vec{v}_{20}^{iT}\tilde{\omega}_{20}^i\vec{r}_2^{Ci}\\
&\quad - m_2^i g\vec{u}_3^T\left\{\vec{r}_{10}^i + p_{20}^T\vec{r}_2^{Ci}\right\}\\
&\quad (i = A, B, C,\ \ p = a, b, c).
\end{aligned}
\tag{26}
$$

The first derivatives of orthogonal matrices $p_{k,k-1}$ are expressed as follows:

$$
\begin{aligned}
&\dot{p}_{k,k-1} = \dot{\varphi}_{k,k-1}^i\tilde{u}_3^T p_{k,k-1},\ \dot{p}_{k,k-1}^T = \dot{\varphi}_{k,k-1}^i p_{k,k-1}^T\tilde{u}_3,\\
&\frac{\partial p_{k,k-1}}{\partial\varphi_{k,k-1}^i} = \tilde{u}_3^T p_{k,k-1}, \qquad \frac{\partial p_{k,k-1}^T}{\partial\varphi_{k,k-1}^i} = p_{k,k-1}^T\tilde{u}_3.
\end{aligned}
\tag{27}
$$

Now, we can calculate the partial derivatives of the Lagrange functions

$$
\begin{aligned}
&\frac{\partial L_p}{\partial x_0^G} = 0, \qquad \frac{\partial L_p}{\partial y_0^G} = 0, \qquad \frac{\partial L_p}{\partial z_0^G} = -m_p g,\\
&\frac{\partial L_p}{\partial \dot{x}_0^G} = m_p\dot{x}_0^G, \qquad \frac{\partial L_p}{\partial \dot{y}_0^G} = m_p\dot{y}_0^G,\\
&\frac{\partial L_p}{\partial \dot{z}_0^G} = m_p\dot{z}_0^G,\\
&\frac{\partial L_1^i}{\partial\lambda_{10}^i} = -m_1^i g\vec{u}_3^T p_{10}^T\vec{u}_3, \qquad \frac{\partial L_1^i}{\partial\dot{\lambda}_{10}^i} = m_1^i\dot{\lambda}_{10}^i,\\
&\frac{\partial L_2^i}{\partial\lambda_{10}^i} = -m_2^i g\vec{u}_3^T p_{10}^T\vec{u}_3,\\
&\frac{\partial L_2^i}{\partial\dot{\lambda}_{10}^i} = m_2^i\dot{\lambda}_{10}^i + m_2^i\dot{\varphi}_{21}^i\vec{u}_3^T p_{21}^T\tilde{u}_3\vec{r}_2^{Ci},\\
&\frac{\partial L_2^i}{\partial\varphi_{21}^i} = m_2^i\dot{\lambda}_{10}^i\dot{\varphi}_{21}^i\vec{u}_3^T p_{21}^T\tilde{u}_3\tilde{u}_3\vec{r}_2^{Ci} - m_2^i g\vec{u}_3^T p_{20}^T\tilde{u}_3\vec{r}_2^{Ci},\\
&\frac{\partial L_2^i}{\partial\dot{\varphi}_{21}^i} = \dot{\varphi}_{21}^i\vec{u}_3^T\hat{J}_2^i\vec{u}_3 + m_2^i\dot{\lambda}_{10}^i\vec{u}_3^T p_{21}^T\tilde{u}_3\vec{r}_2^{Ci}.
\end{aligned}
\tag{28}
$$

An extensive calculus of the derivatives with respect to time $\frac{d}{dt}\{\frac{\partial L}{\partial\dot{q}_k}\}$ $(k = 1, 2, \ldots, 9)$ of the above functions leads to an algebraic system of nine relations. In the direct or inverse dynamics problem, after elimination of six multipliers, finally we obtain the same expressions (20) for the input forces $f_{10}^A$, $f_{10}^B$, $f_{10}^C$ required by the prismatic actuators.

As an application, let us consider a 3-PRC PKM which has the following characteristics:

$$
\begin{aligned}
&r = 0.152\text{ m}, \qquad l_2 = 0.400\text{ m}, \qquad h = 0.1612\text{ m},\\
&\theta = \frac{\pi}{6}, \qquad l = 2r\sqrt{3}, \qquad \Delta t = 2\text{ s},\\
&l_2\cos(\theta+\beta) = r\sin\theta + h\cos\theta,\\
&l_1 = r\cos\theta - h\sin\theta + l_2\sin(\theta+\beta),\\
&m_1 = 1.297\text{ kg}, \qquad m_2 = 0.906\text{ kg},\\
&m_p = 3.982\text{ kg}, \qquad g = 9.807\text{ ms}^{-2}.
\end{aligned}
\tag{29}
$$

Using the MATLAB software, a computer program was developed to solve the inverse dynamics of the 3-PRC parallel manipulator, supposing that there are no external forces and moments acting on the moving platform. To develop the algorithm, it is assumed that the platform starts at rest from a central configuration and moves pursuing a helical translation. The time-history for displacements $\lambda_{10}^i$ (Fig. 3), angles of rotation $\varphi_{21}^i$ (Fig. 4), input forces $f_{10}^i$ (Fig. 5) and powers $P_{10}^i$ (Fig. 6) of three actuators are illustrated for a period of $\Delta t = 2$ seconds in terms of given analytical equations (4).

Since the intermediate limbs connecting the moving platform can be manufactured with light materi-

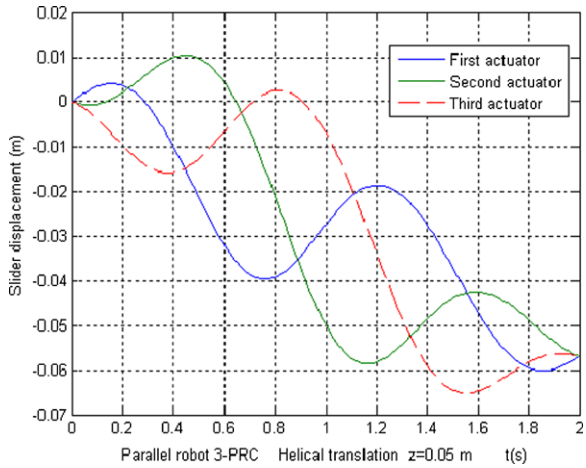


**Fig. 3** Displacements $\lambda_{10}^i$ of three sliders

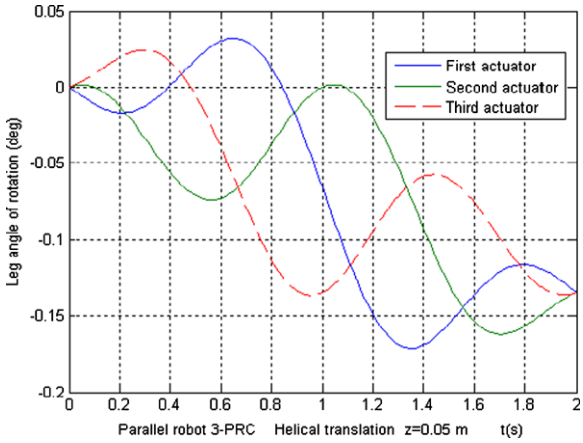


**Fig. 4** Rotation angles $\varphi_{21}^{i}$ of three legs

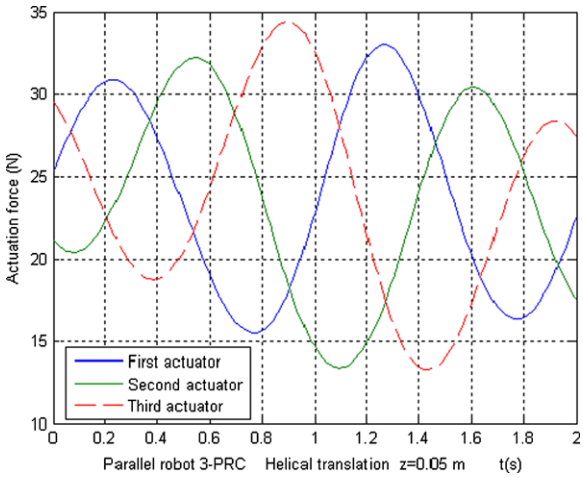


**Fig. 5** Input forces $f_{10}^{i}$ of three actuators

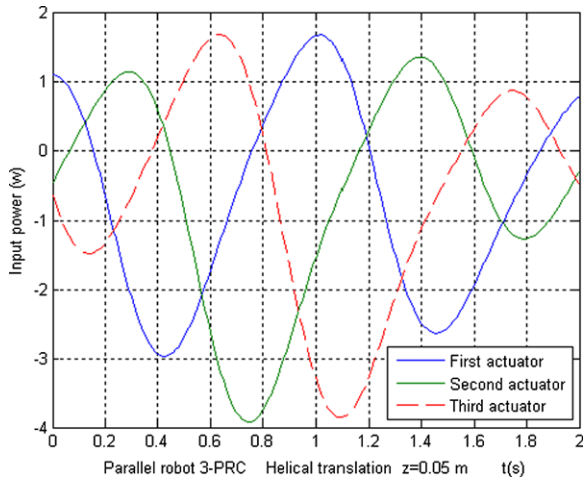


**Fig. 6** Powers $P_{10}^{i}$ of three actuators

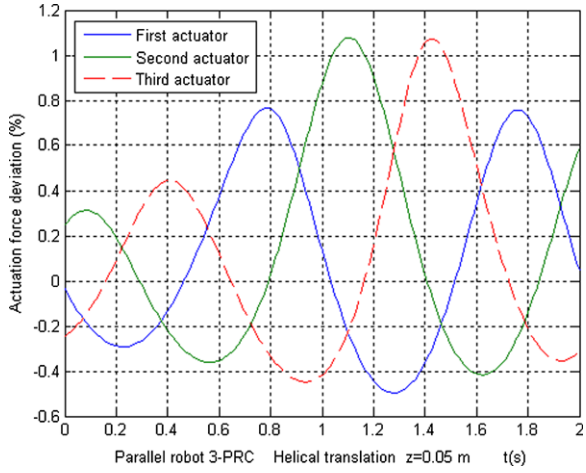


**Fig. 7** Error-coefficients $\Delta f_{10}^{i}$ of three actuators

als, we can *simplify* the dynamics analysis by defining a mass distribution factor $w$ $(0 < w < 1)$ for the legs. That is, the mass of each limb is divided into two portions and placed at its two extremities (Fig. 2), i.e., one part with the proportion of $w$ at its upper extremity (cylindrical joint) and the other part $1 - w$ at its lower extremity (slider). Hence, the rotational inertias of these rods are neglected assuming that the mass of each connecting rod is divided evenly and concentrated at its two extremities.

Pursuing this simplifying hypothesis, a comparative study of two sets of actuation forces, $f_{10}^{A}$, $f_{10}^{B}$, $f_{10}^{C}$ and $f_{10}^{A*}$, $f_{10}^{B*}$, $f_{10}^{C*}$, obtained using the principle of virtual work, is plotted graphically through the relative error-coefficient $\Delta f_{10}^{i}$ for the actuation force deviation:

$$\Delta f_{10}^{i} = \frac{f_{10}^{i} - f_{10}^{i*}}{f_{10}^{i}} \times 100 \quad (i = A, B, C). \tag{30}$$

From the simulation results for $w = 0.5$ (Fig. 7), we can see that a deviation exists between the exact modelling and the simplifying procedure. The simplified analysis is the consequence of expressing the geometrical constraint conditions in a reduced form, which are obtained from the remark that the distance between $A_2$ and $A_3$, for example, is always equal to the length $l_2$.

For a second example of simulation with $e = -0.5$, we suppose that the evolution of moving platform is in an opposite sense, when the sliders are moving from the common point to fixed base. In this study case, the

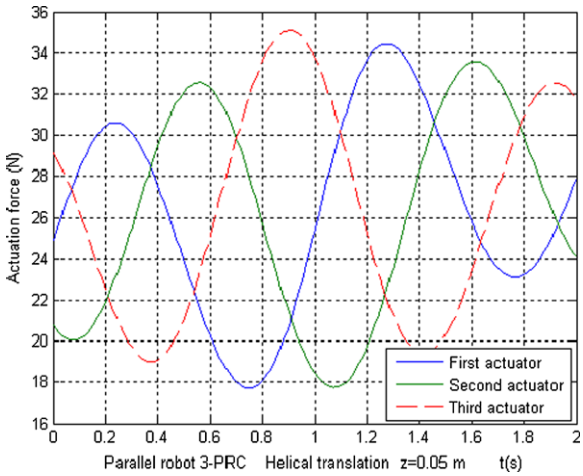


**Fig. 8** Input forces $f_{10}^{i}$ of three actuators

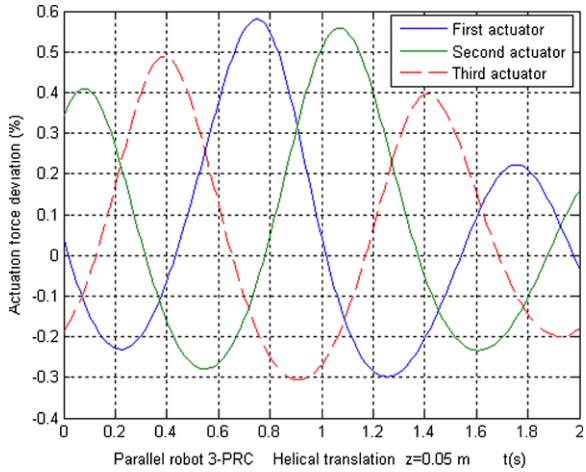


**Fig. 10** Error-coefficients $\Delta f_{10}^{i}$ of three actuators

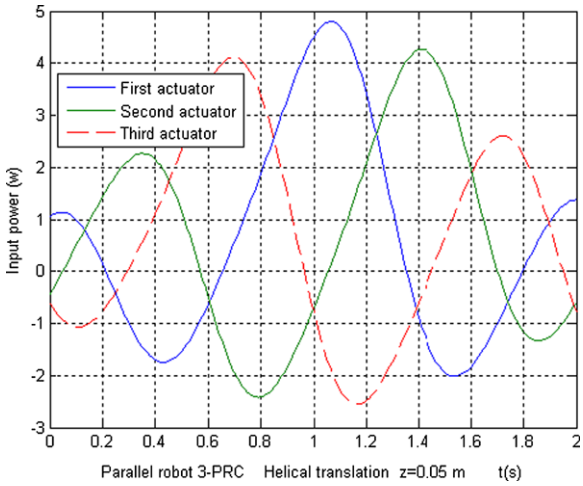


**Fig. 9** Powers $P_{10}^{i}$ of three actuators

forces $f_{10}^{i}$ (Fig. 8), the powers $P_{10}^{i}$ (Fig. 9) and the error-coefficients $\Delta f_{10}^{i}$ (Fig. 10) are again calculated by the program and plotted versus time.

The simulation through the program certifies that one of the major advantages of the current matrix recursive formulation is accuracy and a reduced number of additions or multiplications and consequently a smaller processing time of numerical computation.

## 4 Conclusions

Most of dynamical models based on the Lagrange formalism neglect the weight of intermediate bodies and take into consideration of the active forces or moments only and the wrench of applied forces on the moving platform. Also, the analytical calculations involved in these equations present a risk of errors. The commonly known Newton–Euler method, which takes into account the free-body-diagrams of the mechanism, leads to a large number of equations with unknowns including also the connecting forces in the joints.

With the inverse kinematic analysis, some exact relations that give in real time the position, velocity and acceleration of each element of the parallel robot have been established in the present paper. The dynamics model takes into consideration the mass, the tensor of inertia and the action of weight and inertia force introduced by all compounding elements of the parallel mechanism.

Based on the principle of virtual work, this approach can eliminate all forces of internal joints and establishes a direct determination of the time-history evolution of forces required by the actuators. Choosing appropriate serial kinematical circuits connecting many moving platforms, the present method can easily be applied in forward and inverse mechanics of various types of parallel mechanisms, complex manipulators of higher degrees of freedom and particularly *hybrid structures*, when the number of components of the mechanisms is increased.

**Acknowledgement** The authors appreciate the fund support from the Macao Science and Technology Development Fund under Grant 016/2008/A1.

## References


1. Tsai, L.-W.: Robot Analysis: The Mechanics of Serial and Parallel Manipulators. Wiley, New York (1999)
2. Merlet, J.-P.: Parallel Robots. Kluwer Academic, Dordrecht (2000)
3. Stewart, D.: A platform with six degrees of freedom. Proc. Inst. Mech. Eng., Part I **180**(15), 371–386 (1965)
4. Di Gregorio, R., Parenti Castelli, V.: Dynamics of a class of parallel wrists. J. Mech. Des. **126**(3), 436–441 (2004)
5. Clavel, R.: Delta: A fast robot with parallel geometry. In: Proc. of 18th Int. Symp. on Ind. Robots, Lausanne, pp. 91–100 (1988)
6. Tsai, L.-W., Stamper, R.: A parallel manipulator with only translational degrees of freedom. In: ASME Des. Eng. Tech. Conf., Irvine, CA (1996)
7. Staicu, S.: Recursive modelling in dynamics of Delta parallel robot. Robotica, 199–207 (2009)
8. Hervé, J.-M., Sparacino, F.: Star: A new concept in robotics. In: Proc. of the 3rd Int. Workshop on Advances in Robot Kinematics, Ferrara, pp. 176–183 (1992)
9. Angeles, J.: Fundamentals of Robotic Mechanical Systems: Theory, Methods and Algorithms. Springer, New York (2002)
10. Wang, J., Gosselin, C.: A new approach for the dynamic analysis of parallel manipulators. Multibody Syst. Dyn. **2**(3), 317–334 (1998)
11. Staicu, S.: Recursive modelling in dynamics of Agile Wrist spherical parallel robot. Robot. Comput.-Integr. Manuf. **25**(2), 409–416 (2009)
12. Li, Y.-W., Wang, J., Wang, L.-P., Liu, X.-J.: Inverse dynamics and simulation of a 3-DOF spatial parallel manipulator. In: Proc. of the IEEE Int. Conf. on Robot. & Autom., Taipei, Taiwan, pp. 4092–4097 (2003)
13. Dasgupta, B., Mruthyunjaya, T.S.: A Newton–Euler formulation for the inverse dynamics of the Stewart platform manipulator. Mech. Mach. Theory **34**, 1135–1152 (1998)
14. Khalil, W., Ibrahim, O.: General solution for the dynamic modelling of parallel robots. In: Proc. of the IEEE Int. Conf. on Robot. & Autom., New Orleans, pp. 3665–3670 (2004)
15. Li, Y., Xu, Q.: Kinematics and inverse dynamics analysis for a general 3-PRS spatial parallel mechanism. Robotica **23**(2), 219–229 (2005)
16. Geng, Z., Haynes, L.S., Lee, J.D., Carroll, R.L.: On the dynamic model and kinematic analysis of a class of Stewart platforms. Robot. Auton. Syst. **9** (1992)
17. Miller, K., Clavel, R.: The Lagrange-based model of Delta-4 robot dynamics. Robotersysteme **8**, 49–54 (1992)
18. Zhang, C.-D., Song, S.-M.: An efficient method for inverse dynamics of manipulators based on virtual work principle. J. Robot. Syst. **10**(5), 605–627 (1993)
19. Song, Y., Li, Y., Huang, T.: Inverse dynamics of a 3-RPS parallel mechanism based on virtual work principle. In: Proc. of the 12th IFToMM World Congress, Besançon, France (2007)
20. Sokolov, A., Xirouchakis, P.: Dynamics of a 3-DOF parallel manipulator with R-P-S joint structure. Mech. Mach. Theory **42**, 541–557 (2007)
21. Tsai, L.-W.: Solving the inverse dynamics of Stewart–Gough manipulator by the principle of virtual work. ASME J. Mech. Des. **122** (2000)
22. Yun, Y., Li, Y.: Design and analysis of a novel 6-DOF redundant actuated parallel robot with compliant hinges for high precision positioning. Nonlinear Dyn. **61**(4), 829–845 (2010)
23. Liu, Y., Li, Y.: Dynamic modelling and adaptive neural-fuzzy control for nonholonomic mobile manipulators moving on a slope. Int. J. Contr. Autom. Syst. **4**(2), 197–203 (2006)
24. Yao, B., Xu, L.: Output feedback adaptive robust control of uncertain linear systems. J. Dyn. Syst. Meas. Control **128**(4), 938–945 (2006)
25. Li, Y., Xu, Q.: Kinematic analysis of a 3-PRS parallel manipulator. Robot. Comput.-Integr. Manuf. **23**(4), 395–408 (2007)
26. Li, Y., Xu, Q.: Kinematic analysis and design of a new 3-DOF translational parallel manipulator. J. Mech. Des. **128**(4), 729–737 (2006)
27. Xu, Q., Li, Y.: Investigation on mobility and stiffness of a 3-DOF translational parallel manipulator via screw theory. Robot. Comput.-Integr. Manuf. **24**(3), 402–414 (2008)
28. Staicu, S., Zhang, D.: A novel dynamic modelling approach for parallel mechanisms analysis. Robot. Comput.-Integr. Manuf. **24**(1), 167–172 (2008)
29. Li, Y., Xu, Q.: Dynamic modelling and robust control of a 3-PRC translational parallel kinematic machine. Robot. Comput.-Integr. Manuf. **25**, 630–640 (2009)
30. Staicu, S., Liu, X.-J., Wang, J.: Inverse dynamics of the HALF parallel manipulator with revolute actuators. Nonlinear Dyn. **50**(1–2), 1–12 (2007)
31. Yang, G., Chen, I.-M., Lin, W., Angeles, J.: Singularity analysis of three-legged parallel robots based on passive-joint velocities. IEEE Trans. Robot. Autom. **17**(4), 413–422 (2001)
32. Liu, X.-J., Zin, Z.-L., Gao, F.: Optimum design of 3-DOF spherical parallel manipulators with respect to the conditioning and stiffness indices. Mech. Mach. Theory **35**(9), 1257–1267 (2000)
33. Xi, F., Zhang, D., Mechefske, C.M., Lang, S.Y.T.: Global kinetostatic modelling of tripod-based parallel kinematic machine. Mech. Mach. Theory **39**(4), 357–377 (2001)
34. Bonev, I., Zlatanov, D., Gosselin, C.: Singularity analysis of 3-DOF planar parallel mechanisms via screw theory. J. Mech. Des. **25**(3), 573–581 (2003)
35. Bi, Z.M., Lang, S.Y.T., Verner, M.: Dynamic modelling and validation of a tripod-based machine tool. Int. J. Adv. Manuf. Technol. **37**(3–4), 410–421 (2008)
36. Staicu, S., Liu, X.-J., Li, J.: Explicit dynamics equations of the constrained robotic systems. Nonlinear Dyn. **58**(1–2), 217–235 (2009)
37. Staicu, S.: Dynamics analysis of the Star parallel manipulator. Robot. Auton. Syst. **57**(11), 1057–1064 (2009)
38. Lu, Y., Hu, B., Yu, J.P.: Unification and simplification of dynamics of limited-DOF parallel manipulators with linear active legs. Int. J. Robot. Autom. **25**(2), 45–53 (2010)
39. Hu, B., Lu, Y., Yu, J.P.: Analysis dynamics of some limited-DOF parallel manipulators with $n$ UPS active legs and a passive constraining leg. Adv. Robot. **24**(7), 1003–1016 (2010)